Heliyon

Received:
9 November 2018
Revised:
15 March 2019
Accepted:
12 April 2019

Cite as:
Mary Jenisha Barnabas, Surendran Parambadath, Saravanan Nagappan, Chang-Sik Ha. Sulfamerazine Schiff-base complex intercalated layered double hydroxide: synthesis, characterization, and antimicrobial activity. Heliyon 5 (2019) e01521.
doi: 10.1016/j.heliyon.2019.e01521

Sulfamerazine Schiff-base complex intercalated layered double hydroxide: synthesis, characterization, and antimicrobial activity

Mary Jenisha Barnabas, Surendran Parambadath, Saravanan Nagappan, Chang-Sik Ha*

Department of Polymer Science and Engineering, Pusan National University, Geumjeong-gu, Busan, 46241, Republic of Korea

* Corresponding author.
E-mail address: csha@pnu.edu (C.-S. Ha).

Abstract

Cobalt (Co(II)) and copper (Cu(II)) complexes of sulfamerazine-salicylaldehyde (SS) ligand intercalated Mg/Al-layered double hydroxide [Co-SS-LDH/Cu-SS-LDH] were prepared for the antimicrobial application. Sulfamerazine and salicylaldehyde were mixed together and dissolved in methanol for the synthesis of SS ligand and modified further by the complexation with Co(II) and Cu(II) metal ions [Co-SS/Cu-SS]. The delaminating/restacking method was used to intercalate the Mg/Al-NO_3-LDH with the metal complexed ligands (Co-SS/Cu-SS). The obtained materials were analyzed using different characterization techniques to prove their successful synthesis and preparation. The antibacterial activity of the synthesized Co-SS-LDH/Cu-SS-LDH were checked by the inhibition zone method. The prepared hybrid materials showed good antimicrobial activity against both gram negative (*Escherichia coli, E. coli*) and gram positive (*Staphylococcus aureus, S. aureus*) bacteria.

Keywords: Materials science, Materials chemistry, Inorganic chemistry, Chemical engineering

https://doi.org/10.1016/j.heliyon.2019.e01521

1. Introduction

Layered double hydroxides (LDHs) are a type of bidimensional solids, which have plenty of positive charge in their brucite-like layers [1]. In addition, LDHs are also familiar as anionic clays as well as hydrotalcite-like compounds [1, 2]. LDHs showed potential usage in various applications in recent years owing to their excellent recycling capability and the presence of large interlayer surface with a large pore volume and high specific surface area as well as their easy preparation ways [1, 2]. LDHs possess the skeletal structure, $[M^{2+}_{1-x}M^{3+}_{x}(OH)_2]$ $(A^{m-})_{x/m}\cdot nH_2O$ (M^{2+} = Mg^{2+}, Zn^{2+}, Ni^{2+} etc., M^{3+} = Al^{3+}, Cr^{3+}, Ga^{3+}etc.), where A^{m-} is the interlayer anions, like NO^{3-}, $CO_3{}^{2-}$, and $SO_4{}^{2-}$, and x is in the range of 0.17−0.33 [2]. The introduction of anions (together with water) in the interlayer space would compensate the excess charge, which is developed by an exchange of a divalent cation with a trivalent cation [2, 3, 4]. The interlayer anions can be exchanged with other anions because they are easily exchangeable, which is the most outstanding characteristics of LDHs and can offer high anion exchange capability [1]. In this way, LDHs can be used for the adsorption of metal cations from aqueous solution in spite of the positive charge present in the surface layer [5].

Sulfamerazine is a type of sulfa drug used widely as the preventive and therapeutic compounds against various bacterial infections, such as urinary tract infections, eye infections, actinomics infections, meningitis, and influenza [6, 7]. In addition, sulfamerazine can also be worked as classic compounds to probe the mechanisms of the action of drugs. Better complexing ability and biological activity can be secured by merging products of sulfa drugs with aldehydes, ketones or their derivatives [8]. Similarly, the biological activity can also be improved by complexation with metal ions. A compound possessing of heterocyclic ring system with both nitrogen and sulfur in their structure shows excellent biologically active property [8]. Schiff base ligands are treated as a powerful ligand, due to the ease of preparation as well as one-pot condensation of primary amines and aldehydes in an alcohol solvent [8, 9]. Schiff bases are used widely in various fields, such as intermediates in organic synthesis, biological, catalysis, dyes, polymer stabilizers, and pigments [10, 11]. The complexation of these ligands with metal are ubiquitous because of their apparent synthesis, potentiality for various chemical modifications, and wide applications. In particular, Schiff bases and/or their metal complexes are reported to possess a broad range of biological activities, such as antibacterial, antifungal, antipyretic, anti-inflammatory, antimalarial, antiviral, and anti-proliferative activity [12, 13, 14, 15]. Various kinds of antibacterial agents have been disclosed in the past two decades [16].

Intercalation is an eminent approach used for the inclusion of diverse organic compounds into the interlayer of hydrotalcite-like compounds or anionic clay for a

https://doi.org/10.1016/j.heliyon.2019.e01521

variety of applications. The usability of guest molecules can be expanded by the intercalation of metal-containing anions in the interlayer space of hydrotalcite. The LDH nanocarrier modified materials showed excellent compatibility to cell tissues and sustained delivery behavior [17, 18]. Recently, the synthesis of LDH-indole acetic acid-liposome material showed the potential usage in photodynamic therapy against skin melanoma [19]. Furthermore, the material displayed biodegradable and biocompatible properties and also sustained drug delivery behaviour to various drug molecules. Several research works also focused on the examination of biomolecule incorporated-LDH hybrid materials for biological applications [20, 21]. Furthermore, these drug loaded LDH composites exhibit high chemical stability. Therefore, the Schiff base-intercalated LDH is being a hot topic for developing a novel material with antimicrobial activity and other related biomedical applications. In this work, we report the potential use of the Schiff base ligand based metal-LDH hybrid for antibacterial application.

2. Experimental

2.1. Materials

Magnesium nitrate hexahydrate ($Mg(NO_3)_2 \cdot 6H_2O$), aluminum nitrate nonahydrate ($Al(NO_3)_3 \cdot 9H_2O$), cobalt(II) nitrate hexahydrate ($Co(NO_3)_2 \cdot 6H_2O$), copper(II) nitrate trihydrate ($Cu(NO_3)_2 \cdot 3H_2O$), sulfamerazine, salicylaldehyde, and formamide were obtained from Sigma-Aldrich. Sodium hydroxide (NaOH, 97%) was purchased from Junsei Chemical Co. Ltd. All the chemicals were used as received. The pertinent volume of 2 M NaOH was used to control the pH of the solution.

2.2. Synthesis of [N-(salicylidene)-sulfamerazine] (SS)

Salicylaldehyde (1.22 g, 10 mmol) dissolved in absolute ethanol (50 mL) was added drop-wise with stirring to a solution of sulfamerazine (2.64 g, 10 mmol) in absolute ethanol (50 mL) in a 250 ml round flask. A yellow-colored solution was obtained by heating the reaction mixture under reflux for 6 h, followed by isolating the solid product [8]. The obtained product was filtered and recrystallized by ethanol. Yield: 58 %. m.p. = 215 °C (see Fig. 1). Anal. Calcd. For $C_{18}H_{26}O_3N_4S_1$ (%): C, 57.14; H, 6.87; O, 12.70; N, 14.81; S, 8.46. Found: C, 57.42; H, 6.95; N, 14.88; S, 8.51.

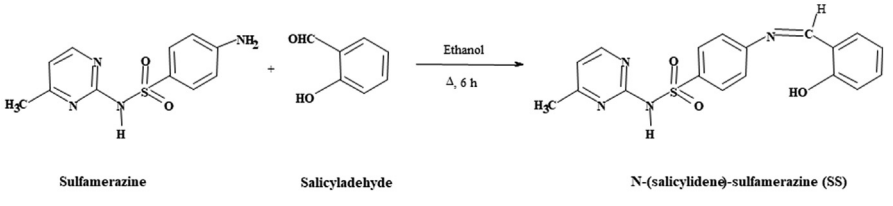

Fig. 1. Preparation of salicylaldehyde-sulfamerazine Schiff base ligand (SS).

https://doi.org/10.1016/j.heliyon.2019.e01521

2.3. Synthesis of Co-SS and Cu-SS complexes

The Schiff base ligand metal complexes were obtained by reacting $Co(NO_3)_2 \cdot 6H_2O$ (0.291 g; 1.0 mmol) and $Cu(NO_3)_2 \cdot 3H_2O$ (0.241 g; 1.0 mmol), with 0.378 g (1 mmol) of Schiff base ligand. First, the Schiff base ligand was prepared separately in absolute ethanol (20 mL), followed by slow addition of metal salts to a solution of the ligand [8]. The reaction mixture was stirred at room temperature for 1 hour. The obtained sample was filtered, washed with ethanol, followed by drying at 50 °C for overnight (see Fig. 2). $Co(C_{18}H_{26}O_3N_4S_1)_2$. Yield (%): 70.72, pink, m.p.: 175 °C, mol. wt.: 624, Anal. Calc. (%): Co, 7.23; C, 53.01; H, 6.38; O, 11.78; N, 13.74; S, 7.85. Found (%): Co, 7.65; C, 53.32; H, 6.87; N, 13.91; S, 7.89. $Cu(C_{18}H_{26}O_3N_4S_1)_2$. Yield (%): 71.33, dark brown, m.p.: 182 °C, mol. wt.: 628, Anal. Calc. (%): Cu, 7.75; C, 52.71; H, 6.34; O, 11.71; N, 13.66; S, 7.81. Found (%): Cu, 7.96; C, 52.86; H, 6.86; N, 13.82; S, 7.99.

2.4. Mg-Al-NO_3-LDH synthesis

Mg-Al-NO_3-LDH was synthesized by using a co-precipitation method according to the reported procedure with slight modifications [22, 23, 24]. A mixed-metal nitrate solution (0.25 M Mg^{2+} and 0.08 M Al^{3+}) was fine-tuned to pH 9−10 with the addition of 2 M NaOH. White precipitate was obtained by heating the reaction mixture at 80 °C for 18 h. The product was filtered and washed using water, followed by subsequent drying at 85 °C, and ground into a fine powder.

2.5. Intercalation of metal complexes into Mg-Al-NO_3-LDH

A translucent colloidal suspension was produced by the addition of Mg/Al-NO_3-LDH sample (0.075 g) into formamide (30 mL), and allowed to keep for 24 h in a stationary condition. 25 mL of ethanol containing Co-SS and Cu-SS complexes (0.3−0.4 g) was added separately to this suspension. During this procedure, the system was changed from translucent to cloudy. The product was stirred vigorously for 24 h, followed by another 48 h of stirring at 70 °C and subsequent cooling to room temperature. The attained materials were named as Cu-SS-LDH and Co-SS-LDH (see Fig. 3).

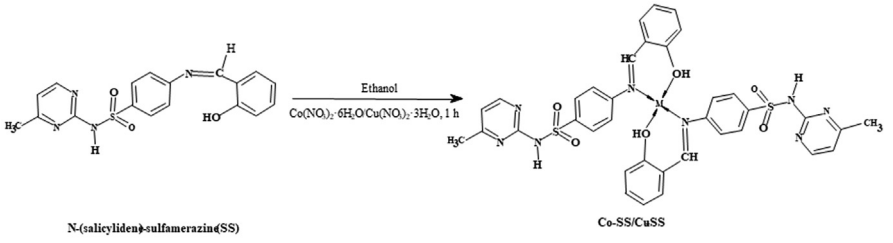

Fig. 2. Preparation of Co(II) and Cu(II) complexes of SS ligand (Co-SS/Cu-SS).

https://doi.org/10.1016/j.heliyon.2019.e01521

2.6. Antimicrobial study

The antimicrobial study was performed according to the standard by the National Committee for Clinical Laboratory Standards (1993a) [25]. The gram-negative *Escherichia coli (E. coli)* and gram-positive *Staphylococcus aureus (S. aureus)* bacteria were used to check the in-vitro antimicrobial screening of the prepared materials. The bacterial culture strains were procured from the Microbial Type Culture Collection and Gene Bank (MTCC) and the standard was referred from the Institute of Microbial Technology (IMTECH), Chandigarh, India. Similar method was used to prepare nutrient agar (NA) as reported in the literature [26]. The sterilized NA medium was solidified on petri dishes. A 100 μL sample of the bacterial cultures (*E. coli* and *S. aureus*) was allowed to grow on the surface of the NA medium. Various concentrations (25, 50 and 100 μg/mL) of the material solutions were prepared in water and loaded onto a sterilized paper disk (diameter: 6 mm) and incubated at 37 °C for 24 h. Water was used to test the antimicrobial activity of the complexes since an organic solvent such as dimethyl formamide was reported to have an inhibitory effect on a bacterial strain such as *Mycobacterium abscessus* unless it is diluted significantly [27]. The inhibition zones appearing around the sample disk were noted as the antibacterial effect of the materials, where the obtained inhibition zone diameters were recorded. The test was carried out for three times in order to obtain an average value.

2.7. Characterization

The X-ray diffraction (XRD) pattern was obtained over the wide angle range from 5° to 70° 2θ by a step scan mode (step size 0.02° with 1s/step of counting time) using powder X-ray diffraction (XRD, Bruker AXN) instrument with Cu-Kα radiation. High resolution scanning electron microscopy (HRSEM, JEOL 6400, 20 kV accelerating voltage) was used for the measurement of the surface morphology of the materials. The materials were loaded on a carbon tape surface, followed by platinum coating before analysis. Transmission electron microscopy (TEM, JEOL 2010, 200 kV accelerating voltage) was also performed. For the TEM measurement,

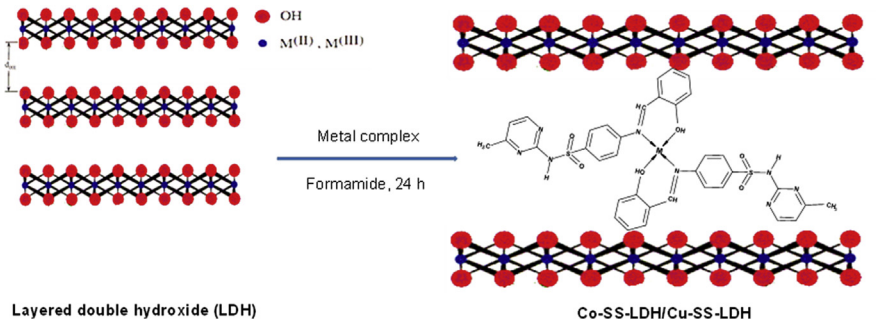

Fig. 3. Intercalation of Co-SS/Cu-SS into layered double hydroxide (Co-SS-LDH/Cu-SS-LDH).

https://doi.org/10.1016/j.heliyon.2019.e01521

samples were dispersed in ethanol and loaded on a copper grid surface by immersion followed by subsequent drying using blown air. Fourier transform infrared (FTIR, JASCO FTIR 4100) spectroscopy was carried out at the frequency range from 400 to 4000 cm^{-1} using the pre-prepared sample using KBr. Thermogravimetric analysis (TGA, Perkin Elmer Pyris Diamond) was conducted at a heating rate of 10 °C min^{-1} in air. The ^{1}H and ^{13}C cross polarization (CP) magic angle spinning (MAS) nuclear magnetic resonance (NMR) (Bruker DSX 400) spectra were recorded using dimethyl sulfoxide (DMSO) with tetramethylsilane (TMS) as the internal standard using a 4 mm zirconia rotor spinning at 6 kHz (resonance frequencies of 79.5 and 100.6 MHz for ^{1}H and ^{13}C CP MAS NMR, respectively). The ultraviolet (UV) absorption spectra of samples in absolute ethanol were observed using a UV-visible spectrophotometer (U- 2010, HITACHI Co.). Elemental analysis was performed using a CHNS analyzer (Carlo Erba Instruments, NQ 1500). The percentages of Co and Cu metal ions in materials were determined by using inductively coupled plasma-optical emission spectrometer (ICP-OES; ACTIVA, JYHORIVA, Japan). Samples were dissolved in hydrogen fluoride prior to measurement.

3. Results and discussion

3.1. Characterization of Mg/Al-NO_3-LDH

The Mg/Al-NO_3-LDH has been already thoroughly studied by many researchers. Thus detailed characterization data of the LDH can be referred to literatures. Only a few fundamental characterization data are presented here, since the LDH synthesized for this work will be used for further complexation with cobalt and copper. Fig. 4a displays the XRD pattern of the Mg/Al-NO_3-LDH, showing intense peaks of (d_{003}), (d_{006}), (d_{009}), (d_{012}), (d_{015}), (d_{110}), and (d_{113}) at 11°, 23°, 34°, 38°, 46°, 61°, and 62° 2θ, respectively [23, 28, 29]. The reflections indexed as the (012), (015), (110), and (113) planes indicate the development of hexagonal lattice with rhombohedral geometry. Several small, rather broad Bragg reflections that are unindexed in the XRD pattern indicate that the Mg/Al-NO_3-LDH synthesized in this work may contain some impurity phase as well as amorphous contents. The FT-IR spectrum of the Mg/Al-NO_3-LDH sample is presented in Fig. 4b. The peak at 1384 cm^{-1} was assigned to the ν_3 vibration of NO_3 [29]. The stretching vibrations of hydroxyl groups and surface and interlayer water molecules were observed as broad and strong bands at 3451 cm^{-1} [23]. The bending mode of water molecules showed a weaker band at 1638 cm^{-1}. The bands at 446 and 672 cm^{-1} were due to Al-O and Mg-O lattice vibrations, respectively [8, 29]. Fig. 4c and d illustrate the HRSEM and TEM images of Mg/Al-NO_3-LDH, respectively. The HRSEM image showed an agglomerated plate-like morphology of the LDH with various particle sizes (diameter: 30−60 nm and 100−500 nm). The TEM image also showed similar plate-like morphology of the LDH with the size of 30−500 nm.

https://doi.org/10.1016/j.heliyon.2019.e01521

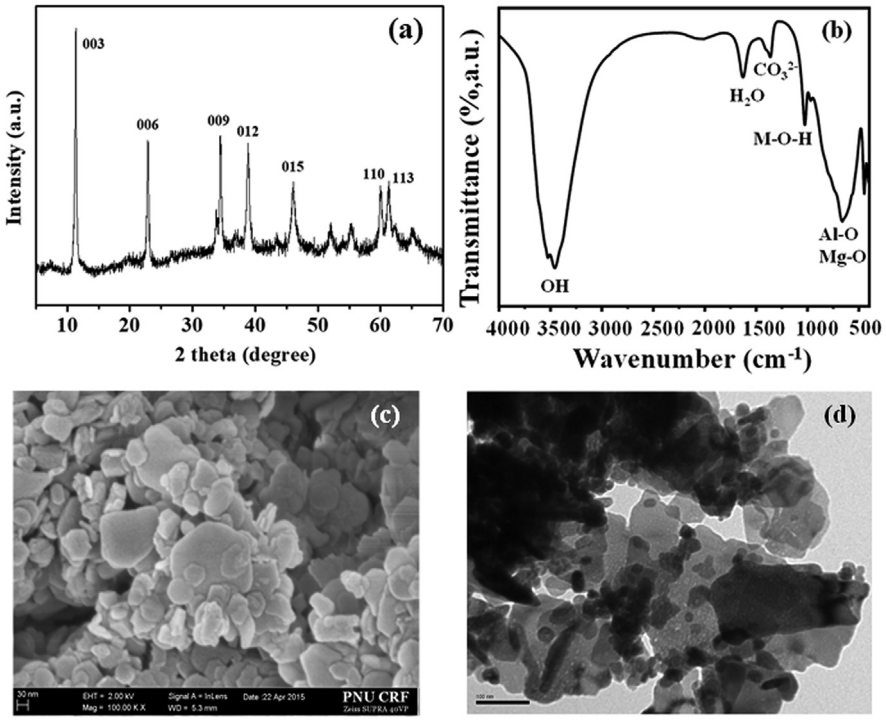

Fig. 4. (a) XRD pattern, (b) FT-IR spectrum, (c) SEM and (d) TEM images of pristine Mg-Al-NO_3-LDH.

3.2. Characterization of Co-SS-LDH and Cu-SS-LDH

3.2.1. XRD analysis

Fig. 5 illustrates the XRD patterns of (a) SS, (b) Co-SS, and (c) Cu-SS. The observed XRD pattern of the SS at 10.4° and 19.8° 2θ are well-matched with previous reports [30, 31]. The loss of free amino groups by reacting the SS with aldehyde and metal ion would lead to reduce the crystallinity. The XRD patterns of Mg-Al-NO_3-LDH, Co-SS-LDH, and Cu-SS-LDH are shown in Fig. 6, where characteristic peaks of Co-SS and Cu-SS as well as LDH were well observed in their XRD patterns when comparing with Fig. 5 [28]. The XRD patterns in Fig. 6, however, clearly show some shifts in the positions of the characteristic crystalline peaks to lower angles and that the intensities of those strong characteristic crystalline peaks of SS, Co-SS, and Cu-SS became weaker and broader. In particular, such shift toward lower angles can be noticeably observed at the low Bragg angles between 5° and 25° 2θ. This result suggests that the Co-SS and Cu-SS was successfully intercalated into the LDH. The d_{003} basal spacing was increased from 8.67Å to 12.43 Å with a gallery height of the intercalated materials of 7.63 Å. Debye-Scherrer equation was used to predict the gallery height from full with half maximum (FWHM) values [32], $D = K\lambda/\beta \cos\theta$, where D is the particle size of the crystal grain; K is a constant

https://doi.org/10.1016/j.heliyon.2019.e01521

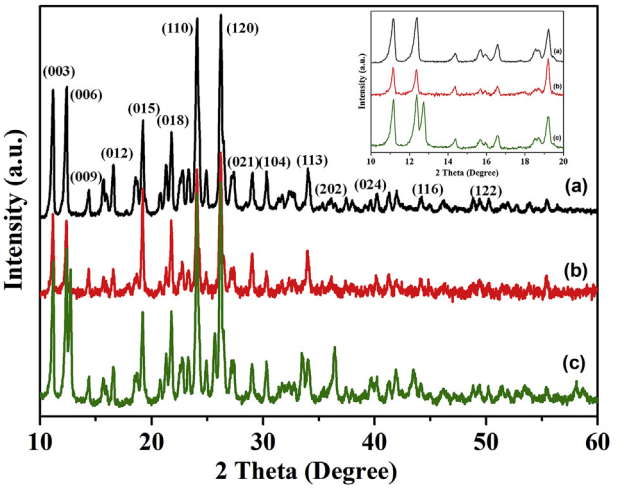

Fig. 5. XRD patterns of (a) SS, (b) Co-SS, and (C) Cu-SS complexes.

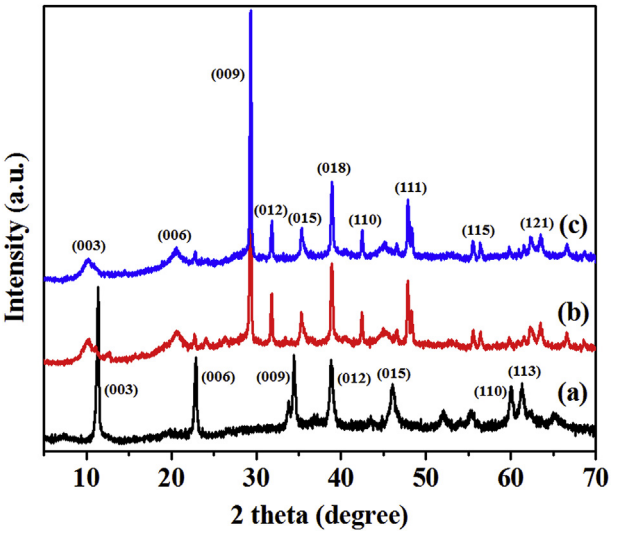

Fig. 6. XRD patterns of (a) Mg-Al-NO_3-LDH, (b) Co-SS-LDH, and (c) Cu-SS-LDH.

(0.94 for Cu grid); λ is the X-ray wavelength (1.5406 Å); and θ and β are the Bragg diffraction angle and integral peak width, respectively. It should be also noted from Fig. 6 that the crystalline peaks of the Co-SS and Cu-SS are maintained even after the intercalation of LDH with Co-SS, and Cu-SS, though some of the crystalline peaks of LDH were overlapped with the Co-SS and Cu-SS peaks. It is considered that the SS is not melting in the organic complex, and moreover the metal ions have strong interactions with the functional groups in SS and form a stable material, as discussed for Fig. 5. The results are attributed to the fact that the anion exchange property of LDH with metal complexed Schiff base can maintain the stability even after intercalation with each other [29].

https://doi.org/10.1016/j.heliyon.2019.e01521

3.2.2. FT-IR analysis

In Fig. 7, the SS ligand showed vibrational bands of -OH, -NH, -CH, C=C, -NH, -C-N-C, and S=O groups, which were remained even after complexation with Co(II) and Cu(II) ions. The peaks at 2999 and 2850 cm^{-1} are due to the asymmetric and symmetric -CH stretching peaks of the methyl group in sulfamerazine. The imino and hydroxyl groups in SS were proved by the broad band at 3440 cm^{-1} [8, 33]. In addition, the FT-IR spectra showed the appearance of N-H bond at 1645 cm^{-1}. The broad peaks at 1160 and 780 cm^{-1} were due to the anti-symmetric stretch of the C-N-C moiety and N-H wagging vibration, respectively. Furthermore, a peak due to the secondary amine was also appeared at 695 cm^{-1} in each spectrum [8, 33]. The new bands in the 550−585 and 430-460 cm^{-1} region noticed for all complexes were assigned to stretching vibrations of (M-O) and (M-N) bonds, respectively. Fig. 8 shows the successful intercalation of Co-SS and Cu-SS complexes in the interlayer cavity of Mg/Al-NO_3-LDH from the existence of the above spectral vibrations with decreased intensities in the spectra, compared to that prior to complexation (as shown in Fig. 7).

3.2.3. ^{1}H NMR and ^{13} C NMR studies

Figs. 9 and 10 illustrate the ^{1}H NMR and ^{13}C NMR spectra of the Schiff base ligand (SS) and diamagnetic complexes (Co-SS and Cu-SS) that were measured in dimethyl sulfoxide (DMSO) with tetramethylsilane (TMS) as the internal standard. The ^{1}H and ^{13}C NMR were run immediately after being dissolved in DMSO and gave the expected simple spectra, indicating the integrity of the Schiff base ligand and complexes. Table 1 lists the ^{1}H NMR spectral data of different protons in the materials.

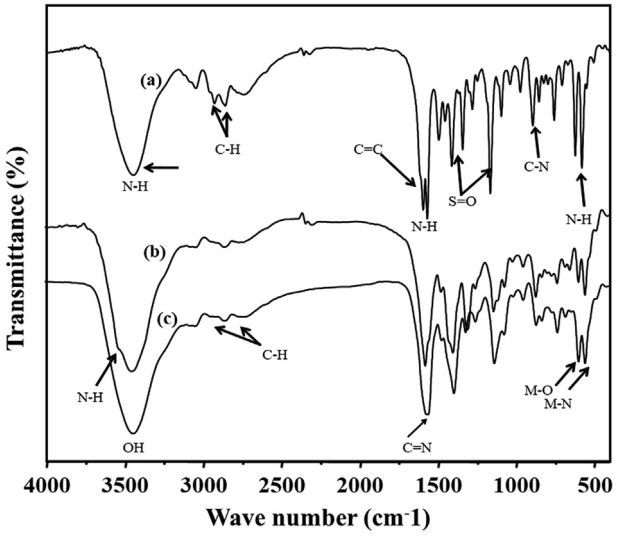

Fig. 7. FT-IR spectra of (a) SS, (b) Co-SS, and (c) Cu-SS complexes.

https://doi.org/10.1016/j.heliyon.2019.e01521

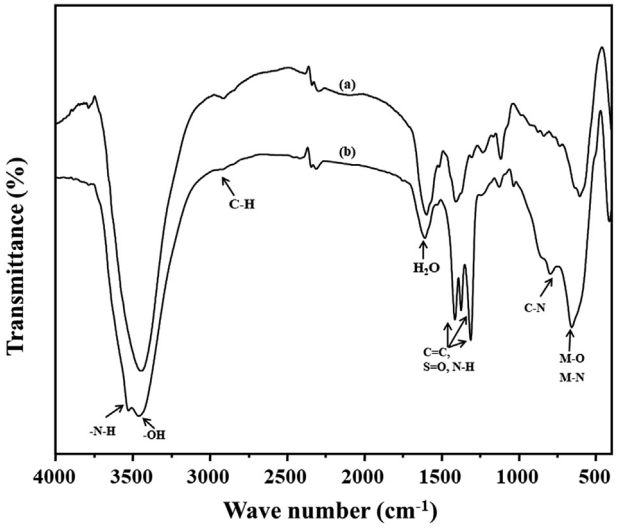

Fig. 8. FT-IR spectra of (a) Co-SS-LDH, and (b) Cu-SS-LDH.

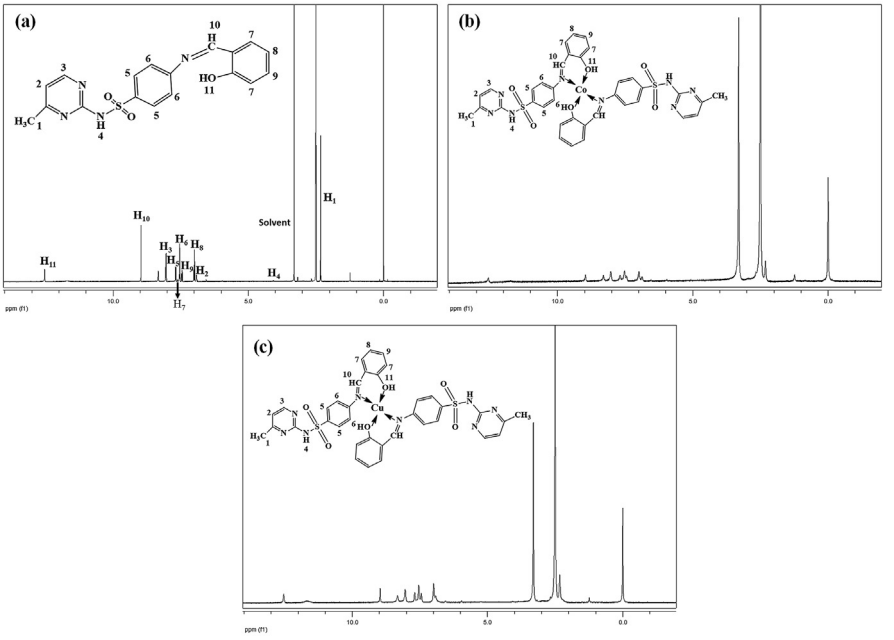

Fig. 9. ^{1} H NMR spectra of (a) SS, (b) Co-SS, and (c) Cu-SS complexes. See Table 1 for the signal assignments.

The imine (CH = N) and O-H protons in the SS-ligand were detected at 8.9 ppm and 12.53 ppm (Fig. 9 and Table 1) [8, 33, 34, 35]. The intensities of imine (CH = N) as well as other aromatic protons peaks were changed partially by complexation with metal, whereas the peak positions are almost identical as in the SS (Table 1) [8, 33, 34, 35]. This reduced peak intensity in the complexes indicates the existence of metal-nitrogen bond. The ^{13}C NMR spectrum of Co-SS-LDH showed several

https://doi.org/10.1016/j.heliyon.2019.e01521

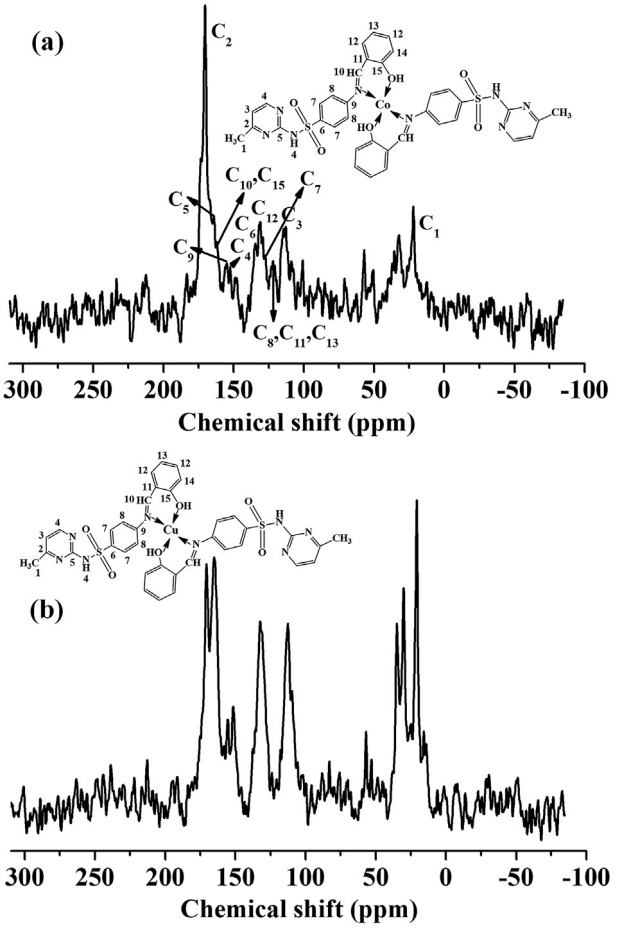

Fig. 10. ^{13} C NMR spectra of (a) Co-SS-LDH and (b) Cu-SS-LDH complex. See Table 1 for the signal assignments.

strong peaks at 170.19, 134.64, 112.85, and 21.99 ppm with some minor peaks, confirming the successful synthesis of the materials (Fig. 10a and Table 1). Similar result was also obtained for Co-SS-LDH with slight modifications in the peak position (Fig. 10b and Table 1).

3.2.4. HRSEM and TEM images

The HRSEM image of Mg/Al-NO_3-LDH showed a plate-like morphology, whereas a sheet-like morphology was observed by intercalating Mg/Al-NO_3-LDH with Co-SS (Fig. 11a). The mean particle size of Co-SS-LDH was in the range of 110−160 nm. The TEM image of the Co-SS-LDH clearly showed uniform distribution of LDH particles in the Co-SS, which suggests appropriate intercalation of the material with each other (Fig. 11b). Fig. 11c and d illustrate the SEM and TEM images of Cu-SS-LDH. Almost identical surface morphology to that of Co-SS-LDH was observed by the introduction of copper instead of cobalt in the hybrid system.

https://doi.org/10.1016/j.heliyon.2019.e01521

Table 1. ^{1}H NMR data for SS, Co-SS, and Cu-SS, and ^{13}C NMR data for C_O-SS-LDH, and Cu-SS-LDH.

^{1}H-NMR (ppm)				^{13}C-NMR (ppm)		
	SS	Co-SS	Cu-SS		Co -SS-LDH	Cu-SS-LDH
H_1	2.31	2.31	2.33	C_1	21.99	20.49
H_2	6.92	6.99	6.99	C_2	170.19	170.63
H_3	8.05	8.05	8.04	C_3	112.85	112.41
H_4	4.01	3.31	4.03	C_4	152.37	151.40
H_5	7.68	7.68	7.68	C_5	164.28	164.72
H_6	7.54	7.51	7.54	C_6	134.64	-
H_7	7.63	7.45	7.42	C_7	127.67	-
H_8	6.99	6.99	6.99	C_8	121.76	124.75
H_9	7.45	7.51	7.51	C_9	155.36	155.37
H_{10}	8.96	8.98	8.97	C_{10}	162.25	158.80
H_{11}	12.53	12.57	12.52	C_{11}	121.76	120.26
				C_{12}	131.20	132.17
				C_{13}	121.76	120.26
				C_{14}	-	118.32
				C_{15}	162.25	158.80

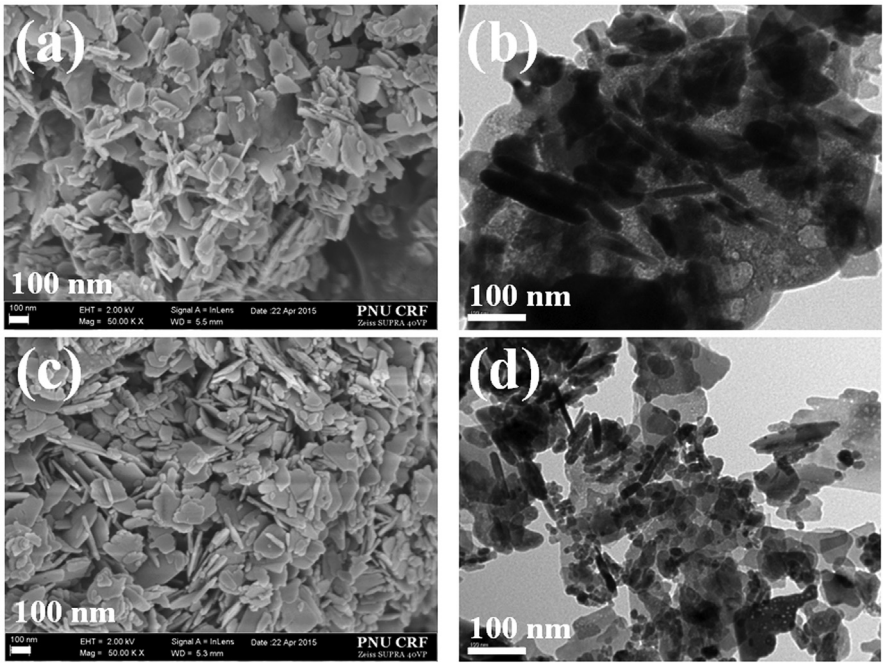

Fig. 11. SEM and TEM images of Co-SS-LDH [(a) and (b)] and Cu-SS-LDH [(c) and (d)], respectively.

https://doi.org/10.1016/j.heliyon.2019.e01521

3.2.5. TGA analysis

Fig. 12 presents the TGA curves of (a) Mg/Al-NO_3-LDH, (b) Co-SS-LDH, and (c) Cu-SSLDH, respectively. As for the previous work, the thermal decomposition behavior of the Mg/Al-NO_3-LDH followed four steps of weight loss including the decomposition of inter layer anions and brucite-like layer as well as the initial weight loss due to the decomposition of physically adsorbed/interlayer structural water molecules in the material [4, 28, 36] (Fig. 12a). The thermal stability of Co-SS-LDH and Cu-SS-LDH are shown in Fig. 12b and c. The materials showed the initial weight loss up to 135 °C, due to the loss of physically adsorbed water molecules (Fig. 12b and c). The organic molecules slowly start to melt and decompose by the increasing the temperature from 135 °C to 330 °C. The 5% and 10% weight loss of the samples were predicted at the temperatures of 90.5 °C and 140 °C for CO-SS-LDH, and 89.2 °C and 146 °C for Cu-SS-LDH, respectively. The decomposition of the organic complex from the intercalated cavity materials was observed in the range 330−450 °C, followed by steady weight loss up to 800 °C (remaining residual mass at 800 °C, 54.4 and 54.7 % for Co-SS-LDH and Cu-SS-LDH, respectively [8]. The organic functional group available in both materials were determined to be approximately 30.5 wt.%. The obtained TGA curves clearly suggest the structural deformation occurred in both materials by intercalation as compared to the pristine LDH.

3.2.6. UV-vis spectroscopy

The UV-vis spectra of Co-SS (Fig. 13Aa) and Cu-SS (Fig. 13Ab) both illustrated two characteristic peaks at 273 and 350 nm, respectively, showing the π-π* and n-π* transitions within the ligand molecule [35]. The Co-SS-LDH (Fig. 13Ba) and Cu-SS-LDH (Fig. 13Bb) exhibited similar absorbance bands. The complex-

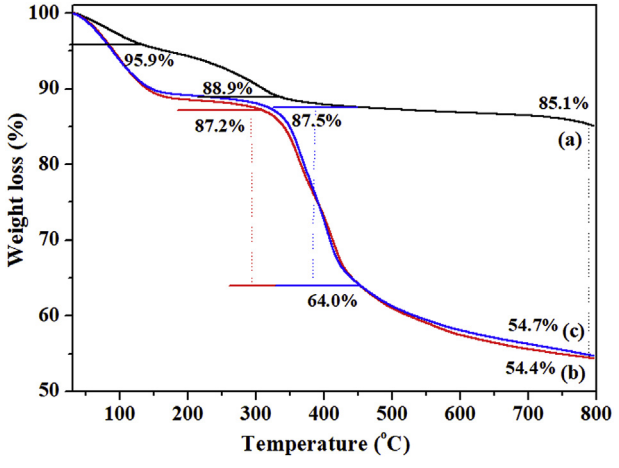

Fig. 12. TGA curves of (a) Mg/Al-NO_3-LDH (b) Co-SS-LDH, and (c) Cu-SS-LDH.

https://doi.org/10.1016/j.heliyon.2019.e01521

intercalated LDH hybrid possess relatively lower abundance compared to the aromatic rings present in the ligand and exhibited less prominent n-π* peak due to the protection by the high reflectance in the visible region. The obtained result proved the intercalation of the complexes into LDH.

3.2.7. Antibacterial properties

An agar disc diffusion method was employed to study the antibacterial activity of both LDH-metal complexes using both *E. coli* and *S. aureus* bacteria. The inhibition zones are illustrated in Fig. 14. The obtained inhibition zones area diameter around the disc was summarized in Table 2. It was reported that the antibacterial activity of LDH could be improved when the pristine LDH is chemically or physically modified [37, 38, 39, 40]. In this work, the results also showed that both Co-SS-LDH and Cu-SS-LDH exhibited much better antibacterial activity against both gram-negative *E. coli* bacteria and gram-positive *S. aureus* than the pristine LDH. The good antibacterial property of the complex-intercalated LDH is due to the release of complexes to the bacterial cell membrane. The interaction of the complexes with the enzyme prosthetic group can inhibit the replication of DNA. It is interesting to note from Table 2

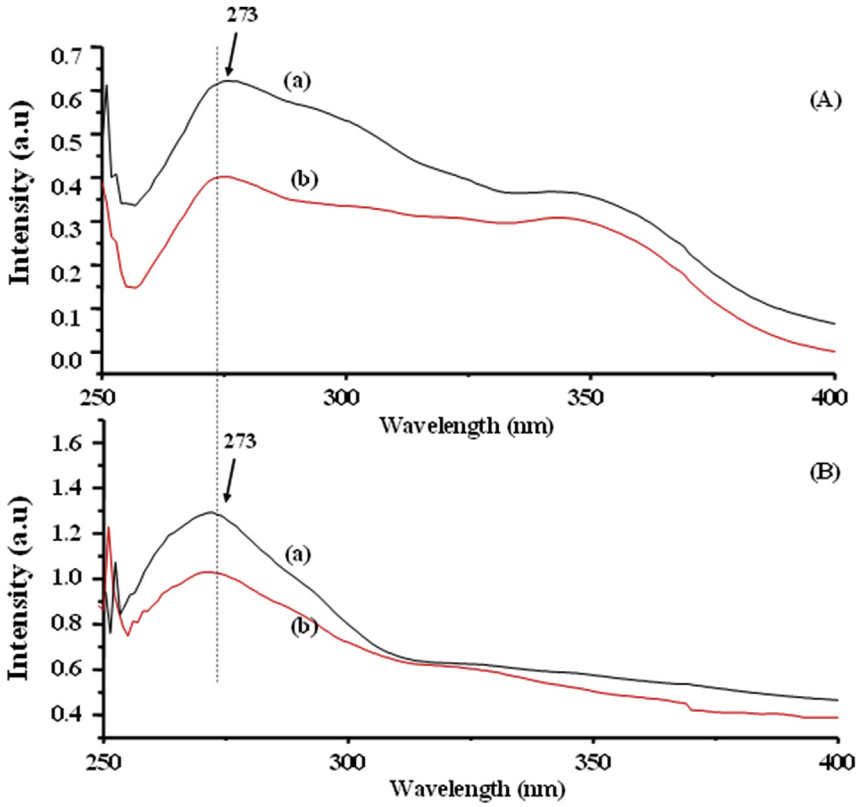

Fig. 13. UV-vis spectra of {[A] Co-SS (a) and Cu-SS (b)} and {[B] Co-SS-LDH (a) and Cu-SS-LDH (b)}.

https://doi.org/10.1016/j.heliyon.2019.e01521

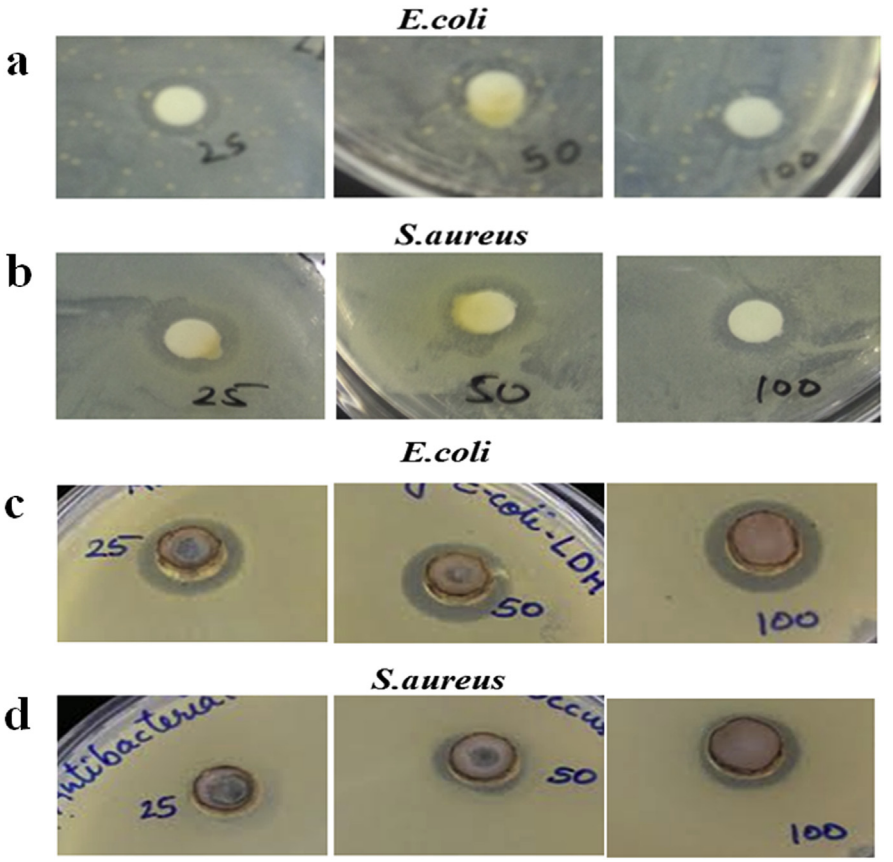

Fig. 14. Antibacterial activity of Co-SS-LDH on (a) *E. coli*, and (b) *S. aureus*, Cu-SS-LDH (c) *E. coli*, and (d) *S. aureus* at various concentrations 25, 50, and 100 μg/ml.

Table 2. Antibacterial activity of Mg-Al-NO_3-LDH, Co-SS-LDH, and Cu-SS-LDH.

Material	Concentration (μg/mL)	Antibacterial activity (mm)	
		E. coli	*S. aureus*
Control*	-	28	28
Mg-Al-NO_3-LDH	25	12	-
	50	13	10
	100	14	12
Co-SS-LDH	25	16	17
	50	17	18
	100	18	18
Cu-SS-LDH	25	19	17
	50	20	18
	100	21	19

* For the control sample, gentamycin was used as a standard antibacterial agent (concentration: 20 mg/mL).

https://doi.org/10.1016/j.heliyon.2019.e01521

that the Cu-SS-LDH showed relatively better antibacterial activity as compared to Co-SS-LDH, while both LDH-metal complexes exhibited marginally higher activity against *E. coli* than *S. aureus*. The change in the structure of the compounds based on the polarity of the metal contents in the complex may be in part the reason behind such difference in the activity of the complexes. The antibacterial activity depends on the sharing nature of the positive charge of the metal with donor groups of the ligands.

4. Conclusions

In this work, we synthesized a new Schiff base ligand followed by the complexation of the ligand with Co(II) and Cu(II) ions. In addition, the Mg/Al-NO_3-LDH was intercalated further with the metal complex. We studied the synthesized materials by various characterization tools and proved the successful formation of the ligand, metal complexes, Mg/Al-NO_3-LDH, and LDH intercalated metal complexes. Furthermore, the antibacterial activity was checked for the pristine Mg/Al-NO_3-LDH and LDH intercalated metal complexes. In conclusion, the obtained results suggest the intercalation of metal complex with the Mg/Al-NO_3-LDH enhances the antibacterial activity of the materials against both gram-negative *E. coli* bacteria and gram-positive *S. aureus* bacteria, suggesting that Co-SS-LDH/Cu-SS-LDH has potential for further biomedical applications. Also, the Cu-SS-LDH exhibited slightly better antibacterial activity for both bacteria as compared to Co-SS-LDH.

Declarations

Author contribution statement

Mary J. Barnabas: Performed the experiments.

Surendran Parambadath, Saravanan Nagappan: Analyzed and interpreted the data; Wrote the paper.

Chang-Sik Ha: Conceived and designed the experiments.

Funding statement

The work was supported by the National Research Foundation of Korea (NRF) grant funded by the Ministry of Science and ICT, Korea {Mid-Career Researcher Program (NRF-2017R1A2B3012961); Brain Korea 21 Plus Program (21A2013800002)}.

Competing interest statement

The authors declare no conflict of interest.

https://doi.org/10.1016/j.heliyon.2019.e01521

Additional information

No additional information is available for this paper.

Acknowledgements

We would like to acknowledge the following foundations such as National Research Foundation of Korea grant funded by the Ministry of Science and ICT, Korea {Mid-Career Researcher Program (NRF-2017R1A2B3012961) and Brain Korea 21 Plus Program (21A2013800002)} for their financial support to carry out this experiment.

References

[1] V. Rives, M.A. Ulibarri, Layered double hydroxides (LDH) intercalated with metal coordination compounds and oxometalates, Coord. Chem. Rev. 181 (1999) 61−120.

[2] F. Cavani, F. Trifiro, A. Vaccari, Hydrotalcite-type anionic clays: preparation, properties and applications, Catal. Today 11 (1991) 173−301.

[3] M.J. Barnabas, S. Parambadath, A. Mathew, S.S. Park, A. Vinu, C.S. Ha, Highly efficient and selective adsorption of In3þ on pristine Zn/Al layered double hydroxide (Zn/Al-LDH) from aqueous solutions, J. Solid State Chem. 233 (2016) 133−142.

[4] M.J. Barnabas, S. Parambadath, C.S. Ha, Amino modified core-shell mesoporous silica based layered double hydroxide (MS-LDH) for drug delivery, J. Ind. Eng. Chem. 53 (2017) 392−403.

[5] J. Gong, T. Liu, X. Wang, X. Hu, L. Zhang, Efficient removal of heavy metal ions from aqueous systems with the assembly of anisotropic layered double hydroxide nanocrystals@carbon nanosphere, Environ. Sci. Technol. 45 (2011) 6181−6187.

[6] B. Aday, P. Sola, F. Çolak, M. Kaya, Synthesis of novel sulfonamide analogs containing sulfamerazine/sulfaguanidine and their biological activities, J. Enzym. Inhib. Med. Chem. 31 (2016) 1005−1010.

[7] Z.H. Chohan, H.A. Shad, Metal-based new sulfonamides: design, synthesis, antibacterial, antifungal, and cytotoxic properties, J. Enzym. Inhib. Med. Chem. 27 (2012) 403−412.

[8] R.C. Maurya, P. Patel, S. Rajput, Synthesis and characterization of mixed-ligand complexes of Cu(II), Ni(II), Co(II), Zn(II), Sm(III), and U(VI)O_2, with a schiff base derived from the sulfa drug sulfamerazine and 2,2′-bipyridine, Syn. React. Inorg. Metal Org. Chem. 33 (2003), 901−816.

https://doi.org/10.1016/j.heliyon.2019.e01521

[9] M. Krátký, M. Dzurková, J. Janoušek, K. Konecná, F. Trejtnar, J. Stolaríková, J. Vinšová, Sulfadiazine salicylaldehyde-based schiff bases: synthesis, antimicrobial activity and cytotoxicity, Molecules 22 (1−15) (2017) 1573.

[10] Y. Jia, J. Li, Molecular assembly of Schiff base interactions: construction and application, Chem. Rev. 115 (2015) 1597−1621.

[11] A.B. Begum, N.D. Rekha, B.C.V. Kumar, V.L. Ranganatha, S.A. Khanum, Synthesis, characterization, biological and catalytic applications of transition metal complexes derived from Schiff base, Bioorg. Med. Chem. Lett. 24 (2014) 3559−3564.

[12] W. Al Zoubi, Biological activities of schiff bases and their complexes: a review of recent works, Int. J. Org. Chem. 3 (2013) 73−95.

[13] B.K. Singh, H.K. Rajour, A. Prakash, Synthesis, characterization and biological activity of transition metal complexes with Schiff bases derived from 2-nitrobenzaldehyde with glycine and methionine, Spectrochim. Acta A 94 (2012) 143−151.

[14] B.S. Creaven, E. Czegledi, M. Devereux, E.A. Enyedy, A.F.-A. Kia, D. Karcz, A. Kellett, S. McClean, N.V. Nagy, A. Noble, A. Rockenbauer, T. Szabo-Planka, M. Walsh, Biological activity and coordination modes of copper(II) complexes of Schiff base-derived coumarin ligands, Dalton Trans. 39 (2010) 10854−10865.

[15] A.K. Mapari, K.V. Mangaonkar, Synthesis, characterization and antimicrobial activity of mixed schiff base ligand complexes of transition metal(II) ions, Int. J. Chem. Tech. Res. 3 (2011) 477−482. ISSN: 0974-4290.

[16] S. Leekha, C.L. Terrell, R.S. Edson, General principles of antimicrobial therapy, Mayo Clin. Proc. 86 (2011) 156−167.

[17] Y. Kuthati, R.K. Kankala, C.H. Lee, Layered double hydroxide nanoparticles for biomedical applications: current status and recent prospects, Appl. Clay Sci. 112−113 (2015) 100−116.

[18] R.K. Kankala, Y. Kuthati, H.W. Sie, H.Y. Shih, S.I. Lue, S.K. Kankala, C.C. Jeng, J.P. Deng, C.F. Weng, C.L. Liu, C.H. Lee, Multi-laminated metal hydroxide nanocontainers for oral-specific delivery for bioavailability improvement and treatment of inflammatory paw edema in mice, J. Colloid Interface Sci. 458 (2015) 217−228.

[19] R.K. Kankala, Y. Kuthati, C.L. Liu, C.H. Lee, Hierarchical coated metal hydroxide nanoconstructs as potential controlled release carriers of photosensitizer for skin melanoma, RSC Adv. 5 (2015) 42666−42680.

https://doi.org/10.1016/j.heliyon.2019.e01521

[20] S.Y. Kwak, Y.J. Jeong, J.S. Park, J.H. Choy, Bio-LDH nanohybrid for gene therapy, Solid State Ionics 151 (2002) 229.

[21] J.H. Choy, J.M. Oh, M. Park, K.M. Sohn, J.W. Kim, Inorganic−biomolecular hybrid nanomaterials as a genetic molecular code system, Adv. Mater. 16 (2004) 1181−1184.

[22] M. Khitous, Z. Salem, D. Halliche, Removal of chromium from synthetic and real effluents using Uncalcined MgAl-NO_3 layered double hydroxide: column study and modeling, J. Sep. Sci. Technol. 50 (2015) 2458−2466.

[23] D. Kostadinova, A.C. Pereira, M. Lansalot, F. D'Agosto, E. Bourgeat-Lami, F. Leroux, C. Taviot-Guého, S. Cadars, V. Prevot, Intercalation and structural aspects of macroRAFT agents into MgAl layered double hydroxides, Beilstein J. Nanotechnol. 7 (2016) 2000−2012.

[24] M. Meyn, K. Benecke, G. Lagally, Anion-exchange reactions of layered double hydroxides, Inorg. Chem. 29 (1990) 5201−5207.

[25] National Committee for Clinical Laboratory Standards, Performance Standards for Antimicrobial Disk Susceptibility Tests—Fifth Edition: Approved Standard M2-A5, NCCLS, Villanova, PA, USA, 1993a.

[26] K.M. Rao, K.S.V. Krishna Rao, G. Ramanjaneyulu, K. Chowdoji Rao, M.C.S. Subha, C.S. Ha, Biodegradable sodium alginate-based semi-interpenetrating polymer network hydrogels for antibacterial application, J. Biomed. Mater. Res. Part A. 102 (2013) 3196−3206.

[27] Z.I. Kirkwood, B.C. Millar, D.G. Downey, E. J, J.E. Moore, Antimicrobial effect of dimethyl sulfoxide and N, N-Dimethylformamide on *Mycobacterium abscessus*: implications for antimicrobial susceptibility testing, Int. J. Mycobacteriol. 7 (2) (2018) 134−136 (2018).

[28] Y. Zhao, F. Li, R. Zhang, D.G. Evans, X. Duan, Preparation of layered double-hydroxide nanomaterials with a uniform crystallite size using a new method involving separate nucleation and aging steps, Chem. Mater. 14 (2002) 4286−4291.

[29] K.M. Parida, M. Sahoo, S. Singha, Synthesis and characterization of a Fe(III)-Schiff base complex in a Zn-Al LDH host for cyclohexane oxidation, J. Mol. Catal. A Chem. 329 (2010) 7−12.

[30] R.S. Joseyphus, M.S. Nair, Synthesis, characterization and biological studies of some Co(II), Ni(II) and Cu(II) complexes derived from indole-3-carboxaldehyde and glycylglycine as Schiff base ligand, Arabian J. Chem. 3 (2010) 195−204.

https://doi.org/10.1016/j.heliyon.2019.e01521

[31] S. Zhang, N. Kano, H. Imaizumi, Synthesis and characterization of LDHs (layered double hydroxides) intercalated with EDTA (Ethylenediaminetetracetic Acid) or EDDS (N, N'-1, 2-ethanediylbis-1-aspartic acid), J. Environ. Sci. Eng. A 5 (2016) 549−558.

[32] P. Scherrer, Bestimmung der Grosse und der Inneren Struktur von Kolloidteilchen Mittels Rontgenstrahlen, Nachrichten von der Gesellschaft der Wissenschaften zu Göttingen, Mathematisch-Physikalische Klasse 2 (1918) 98−100. https://eudml.org/doc/59018.

[33] C.D. Sheela, C. Anitha, P. Tharmaraj, D. Kodimunthri, Synthesis, spectral characterization, and antimicrobial studies of metal complexes of the Schiff base derived from [4-amino-N-guanylbenzene sulfonamide] and salicylaldehyde, J. Coord. Chem. 63 (2010) 884−893.

[34] R.C. Maurya, P. Patel, Synthesis, magnetic and special studies of some novel metal complexes of Cu(II), Ni(II), Co(II), Zn[II), Nd(III), Th(IV), and UO_2(VI) with schiff bases derived from sulfa drugs, viz., Sulfanilamide/Sulfamerazine and o-vanillin, Spectrosc. Lett. 32 (1999) 213−236.

[35] X. Ran, L. Wang, D. Cao, Y. Lin, J. Hao, Synthesis, characterization and in vitro biological activity of cobalt(II), copper(II) and zinc(II) Schiff base complexes derived from salicylaldehyde and D,L-selenomethionine, Appl. Organomet. Chem. 25 (2011) 9−15.

[36] F.A. El-Saied, T.A. Salem, M.M.E. Shakdofa, A.N. Al-Hakimi, A.S. Radwan, Antitumor activity of synthesized and characterized Cu(II), Ni(II) and Co(II) complexes of hydrazone-oxime ligands derived from 3-(hydroxyimino) butan-2-one, Beni-Suef Univ. J. Basic Appl. Sci. 7 (2018) 420−429.

[37] C. Chen, P. Gunawan, X.W. Lou, R. Xu, Silver nanoparticles deposited layered double hydroxide nanoporous coatings with excellent antimicrobial activities, Adv. Funct. Mater. 22 (2012) 780−787.

[38] G. Mishra, B. Dash, S. Pandey, P.P. Mohanty, Antibacterial actions of silver nanoparticles incorporated Zn-Al layered double hydroxide and its spinel, J. Environ. Chem. Eng. 1 (2013) 1124−1130.

[39] M. Wang, Q. Hu, D. Liang, Y. Li, S. Li, X. Zhang, M. Xi, X. Yang, Intercalation of Ga^{3+}-salicylidene-amino acid Schiff base complexes into layered double hydroxides: synthesis, characterization, acid resistant property, in vitro release kinetics and antimicrobial activity, Appl. Clay. Sci. 83 (2013) 182−190.

[40] Y. Wang, D. Zhang, Synthesis, characterization, and controlled release antibacterial behavior of antibiotic intercalated Mg-Al layered double hydroxides, Mater. Res. Bull. 47 (2012) 3185−3194.

https://doi.org/10.1016/j.heliyon.2019.e01521